International Journal of Fatigue 59 (2014) 50–63

Contents lists available at ScienceDirect

International Journal of Fatigue

journal homepage: www.elsevier.com/locate/ijfatigue

An optimal design approach for calibrated rolls with respect to fatigue life

Ž. Domazet [a,*], F. Lukša [a], T. Stanivuk [b]

[a] University of Split, Faculty of Electrical Engineering, Mechanical Engineering and Naval Architecture, Ruđera Boškovića 32, 21000 Split, Croatia
[b] University of Split, Faculty of Maritime Studies, Zrinsko-Frankopanska 38, 21000 Split, Croatia

ARTICLE INFO

Article history:
Received 30 April 2013
Received in revised form 14 September 2013
Accepted 23 September 2013
Available online 14 October 2013

Keywords:
Fatigue
Fatigue life
Shape rolling
Calibrated rolls
Optimization

ABSTRACT

In the hot rolling process calibrated rolls are used for the production of various simple and complex profiles. Main factors influencing the fatigue life of these rolls result from the technological process of the rolling; rolling temperature, rolling speed, roll groove design and turning due to wearing. In order to increase maximum fatigue life of the rolls, as well as to reduce overall energy consumption, increase production and reduce overall costs, an analysis of the influence of these parameters on roll fatigue life has been carried out. Based on this analysis, procedure of optimal design of calibrated rolls with respect to fatigue life is developed. The procedure involves both analytical and experimental methods to determine service loads; numerical analysis of local stresses by finite element method and determination of stress time history of individual local stress and stress spectrum from numerical analysis and pass schedule. The fatigue life estimation is carried out according to the fatigue life stress concept based on the local stress. This paper proves that with the application of this procedure, optimal relation between roll fatigue life and energy consumption can be achieved, as well as more optimal production and overall costs.

1. Introduction

In the hot rolling, main factors influencing the fatigue life of calibrated rolls result from the technological process of the rolling [1]. For a particular rolling mill, fixed input parameters of calibrated rolls design are requested by production: rolling material, the type of rolling line, and initial and final section of the rolled piece. According to these parameters and based on practice and previous experience [2,3], the design engineer constructs pass schedule, roll design and groove distribution. Rolling temperature and rolling speed are important parameters of technological process which have great influence on energy costs and overall production. Turning due to wear is an unwanted phenomenon, which has direct influence on production costs. In order to increase the maximum fatigue life of the rolls, reduce overall energy consumption, increase production and finally to reduce overall costs, an analysis of the influence of these parameters on roll fatigue life has been carried out on 3-high-roughing mill stand in "Steelworks Split".

3-High-roughing mill stand was suitable for hot rolling of the billets with initial cross-section 100 mm square and 3 m initial length in 8 passes. The rolling mill production was 70 billets per hour. The mass of one billet was 230 kg. The rolling material was reinforcement steel mark BSt (Betonstahl) 400 S according to German standard DIN (Deutsches Institut für Normung) 488. The initial temperature of the rolled material in the first pass was 1200 °C. The roll speed was 120 rpm. The total length of the roll was 2300 mm, the roll barrel length was 1400 mm and the roll barrel diameter was 450 mm. The roll machining due to wearing was estimated after 4000 rolling tons of steel. Fig. 1 shows the roll design and groove distribution [4]. Pass shape rolling sequence (pass schedule) between rolls and corresponding grooves are numbered. The pass schedule and corresponding data are shown in Table 1.

The material used for the rolls was nodular graphite cast iron with the pearlitic base with hardness on the roll surface 380 HB. The roll mark was KGR-380-P [5]. Chemical composition of the roll material is shown in Table 2. Fig. 2 shows hardness drop of KGR 380 rolls and metallographic structure of the roll material. Tensile strength of the core is 325–425 MPa and bending strength of the core is 500–700 MPa.

1.1. Service load determination

The main parameter in describing the rolling force is resistance to deformation of rolling material. Resistance to deformation depends on the rolling temperature, deformation speed and deformation size. Fig. 3 shows experimentally obtained diagram of Dinnik [2], deformation resistance of low carbon steel St3 for the draught of 30% and different deformation speed and rolling temperature. For draught different than 30%, value of resistance to deformation

* Corresponding author.
E-mail address: zeljko.domazet@fesb.hr (Ž. Domazet).

0142-1123/$ - see front matter © 2013 Elsevier Ltd. All rights reserved.
http://dx.doi.org/10.1016/j.ijfatigue.2013.09.015

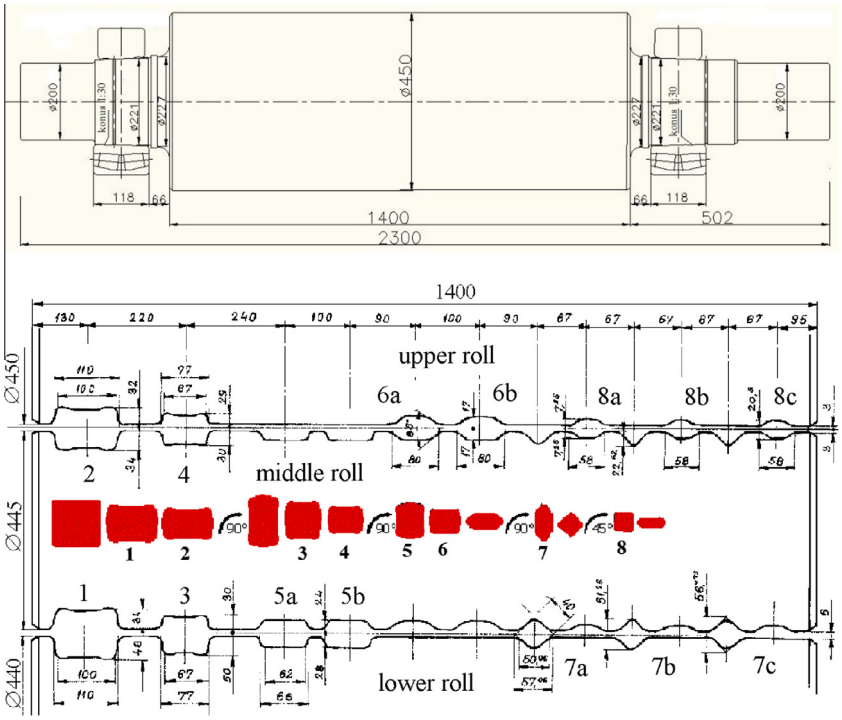

Fig. 1. Roll design and groove distribution.

Table 1
Pass schedule.

Pass		1	2	3	4	5	6	7	8
Pass shape		Box	Box	Box	Box	Box	Oval	Square	Oval
Groove dimensions (mm)		100 × 82	100 × 66	67 × 80	67 × 59	66 × 52	80 × 34	40	58 × 20
Cross-section (mm^2)	9850	8015	6474	5398	4032	3280	2286	1578	1075
Width (mm)	100	104	108	71	76	65	82.5	53.5	60.5
Initial height (mm)		100.0	82.0	108.0	80.0	76.0	52.0	82.5	40.0
Height after pass (mm)		82.0	66.0	80.0	59.0	52.0	34.0	51.0	20.5
Average draught (mm)		17.6	14.3	15.2	18.0	11.6	12.0	13.2	8.3
Absolute reduction (mm^2)		1835	1541	1076	1366	752	994	708	503
Elongation coefficient		1.23	1.24	1.20	1.34	1.23	1.43	1.45	1.47
Working diameter (mm)		372.5	393.5	372.5	398.5	396.5	419.5	397.25	433
Roll speed (rpm)		120	120	120	120	120	120	120	120
Length of rolled stock (m)	3	3.69	4.56	5.47	7.33	9.01	12.93	18.73	27.49
Projected length of arc of contact (mm)		57.84	56.10	72.08	64.68	68.97	61.44	79.10	64.97
Projected area of contact (mm^2)		5900	5947	4938	4754	4276	4531	3461	3265
Rolling speed (ms^{-1})		2.33	2.62	2.42	2.77	2.55	2.78	2.7	2.89
Rolling time (s)		1.58	1.74	2.26	2.65	3.53	4.65	6.92	9.52
Pause (s)		3	3	3	3	3	3	3	3

Table 2
Chemical composition of the rolls [5].

Chemical element	C (%)	Si (%)	Mn (%)	P (%)	S (%)	Cr (%)	Ni (%)	Mo (%)
(%)	3.4–3.6	1.8–2.2	0.5–1	do 0.05	do 0.05	do 0.5	1.5–3	do 0.2

from this diagram should be multiplied by the correction factor a (curve on top of the same diagram).

For rolling sequence in eight passes on 3-high-roughing mill stand, monitoring of rolling temperature was carried out using digital pyrometer. Rolling temperature was in the range between 1200 °C and 1100 °C, see Table 3. Initial temperature in the first pass was 1200 °C. Temperature in eighth pass was 1148 °C. Deformation speeds were determined in accordance with the relation [2]:

$$u = \frac{2v}{h_0 + h_1}\sqrt{\frac{2\Delta h_{sr}}{R_1 + R_2}} \quad (1)$$

where v is the rolling speed, h_0 is the initial height and h_1 is the height after pass, Δh_{sr} is average draught, R_1 and R_2 are radii of rolls, see Table 1. Deformation speed as in the range between 7.4 and 18.7 s^{-1}, see Table 3.

There are numerous formulae for calculating the rolling force in hot rolling. Analytical calculation for this process was done

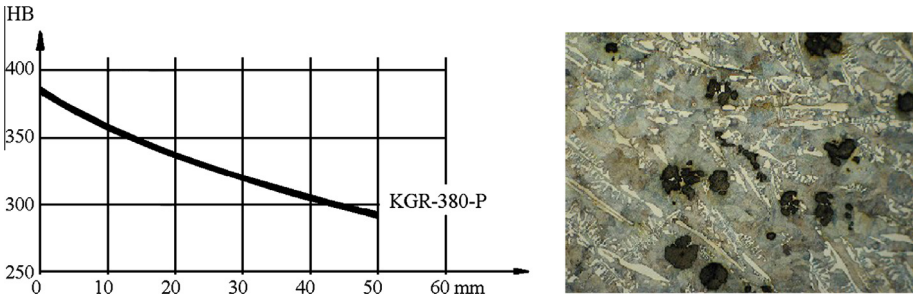

Fig. 2. Hardness drop and metallographic structure (500×) [5].

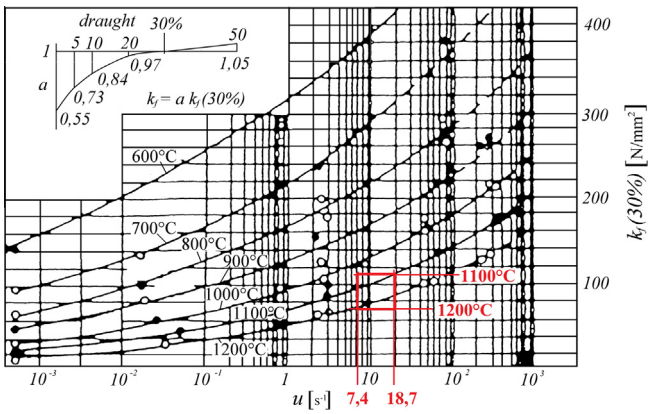

Fig. 3. Resistance to deformation of low carbon steel St3, A.A.Dinnik, [2].

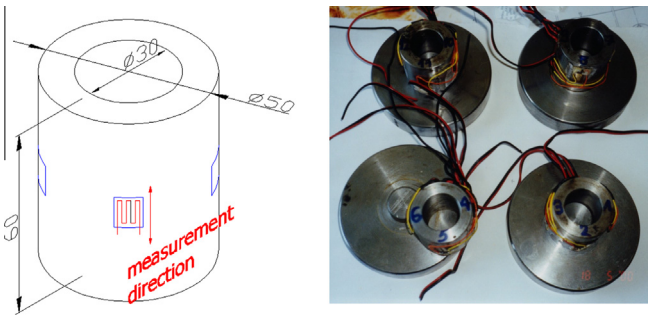

Fig. 4. Load cells.

according to methods of Tselikov, Ekelund, Korolev, Geleji, Golovin and Tiagunov, Sims and Siebel and the results were compared [6]. In analytical calculation according to the Tselikov, Korolev, Sims and Siebel methods, the resistance to deformation was determined using the experimentally obtained diagram of Dinnik, Fig. 3. In the analytical calculation made by the Ekelund, Geleji and Golovin-Tjagunov method, the resistance to deformation was determined in accordance to corresponding expression. The comparison of results showed large deviations, see Fig. 6.

Therefore the rolling forces were determined by experimental testing [7]. In accordance with results from analytical methods for determining the rolling force, four load cells with three strain gauges on each of them were designed for experimental determining of the rolling force, Fig. 4.

The measuring devices were mounted on both sides of the stand, instead of two safety parts against the breakage of rolls, see Fig. 5. One pair of load cells was used to measure reaction forces due to rolling force between two rolls (lower and middle roll or middle and upper roll). The measurement of rolling forces was carried out during the 1 h of rolling production. The monitoring of the rolling temperature was carried out using digital pyrometer. Experimentally determined rolling forces and temperature of the rolling material are shown in Table 3.

Fig. 6 shows the comparison of experimentally determined rolling forces and calculated results according to methods of Tselikov, Ekelund, Korolev, Geleji, Golovin and Tiagunov, Sims and Siebel for rolling in eight passes, see Table 1 and Fig. 1.

It may be seen from the curves shown in Fig. 6 that, for the same rolling conditions, there are large deviations in calculated values of force rolling by different authors. Values obtained for rolling forces calculated according to Tselikov, Korolev, Sims and Siebel have a good agreement with experimentally determined values in the first six passes and the eighth pass and deviations in the seventh pass. The first six passes and the eighth pass have clearly expressed contact surface and the shape is closer to rolling flat profile. In the seventh pass, due to square shape, pressure on the rolls varies considerably due to uneven deformation and additional frictional force on the sides of the caliber. Values obtained for rolling forces calculated according to Ekelund, Geleji and Golovin-Tjagunov methods are too low. Based upon these results, formulae of Tselikov, Korolev, Sims and Siebel will be used in calculation of force for different rolling temperature and rolling speed.

Because of numerous parameters (the properties of rolls and the rolling material; the form of the grooves; the friction between rolls and rolling material...) experimental methods are more suitable and more accurate for determining the rolling force in the grooves.

Table 3
Experimentally determined rolling forces [7].

Pass No.		1	2	3	4	5	6	7	8
Rolling temperature (°C)	1200	1198	1194	1188	1183	1176	1169	1159	1146
Deformation speed (s^{-1})		7.9	9.5	7.4	12	9.6	15.5	10.5	18.7
Experimentally determined rolling forces (kN)		356.1	494.6	356.1	524.2	346.2	544.0	286.8	445.1

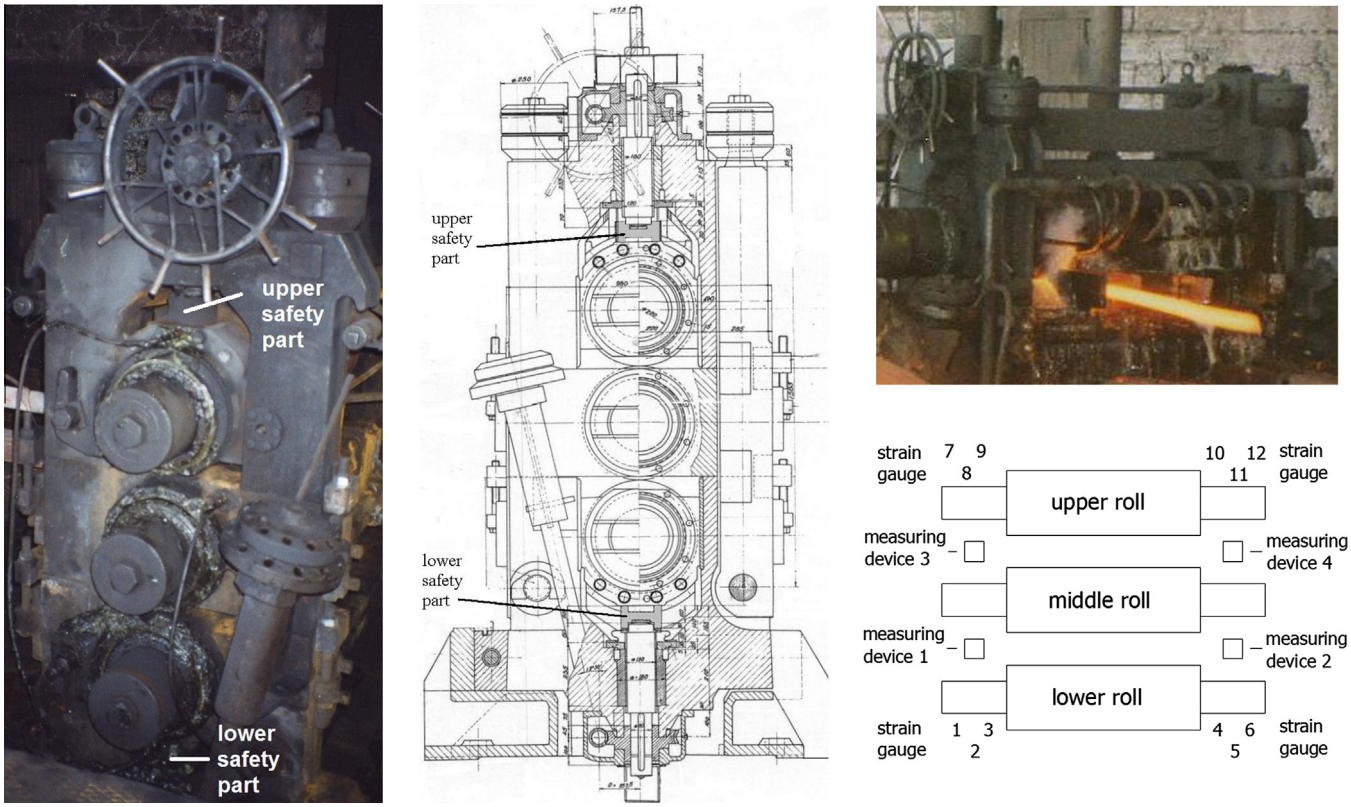

Fig. 5. Positions of load cells on 3-high-roughing mill stand.

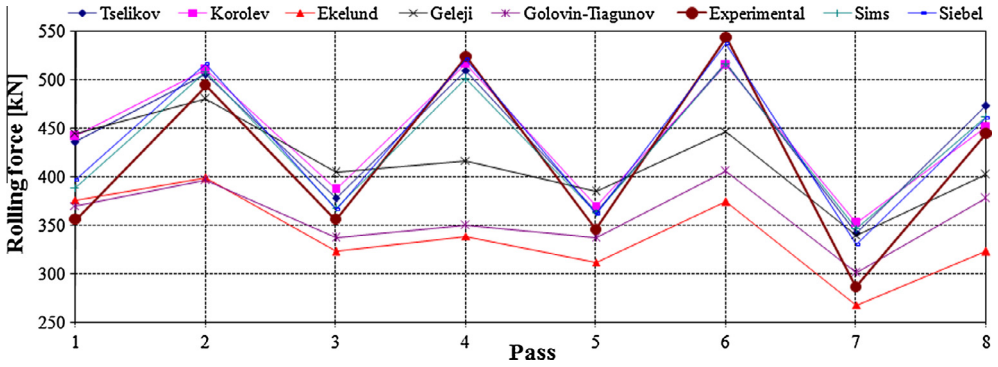

Fig. 6. Analytically and experimentally determined rolling forces.

1.2. Local stress determination

Obtained experimental results of rolling forces are used for the numerical analysis of local stresses by the finite element method using ADINA software. The linear elastic model with 3D solid elements with eight nodes per element was used, Fig. 7. Each node has 3 degrees of freedom, translation in *X*, *Y* and *Z* direction. The model is fixed on the both ends in the line and loaded with concentrated forces in the nodes. In Fig. 7 is shown concentrated force due to rolling force in pass 1.

The complete numerical analysis included 30 cases of loading according to the rolling schedule. The FEM revealed that there are 3 critical areas of the roll: roll neck, pass groove 3–4 and pass groove 7a. Stress concentration factors at the critical areas have a good agreement with literature [8,9]. Fig. 8 shows the FEM model of the middle roll with stock positions in pass grooves 2 and 6 and corresponding stresses in direction *Z*. Critical areas of the roll are marked in figure.

1.3. Stress spectrum determination on critical area

3-High-roughing mill stand rolling diagram according to time is constructed from the mill production and pass schedule, Fig. 9.

Rolling starts with the first billet in the pass 1 and rolling duration is 1.58 s, see Fig. 9. After 3 s of idle time, the rolling stock comes in pass 2 and rolling duration is 1.74 s. Then follow pass 3 and pass 4 and after 20 s of the first stock start, begins the rolling process of two billets together. Then the rolling process on the 3-high-roughing mill stand continues according to rolling schedule.

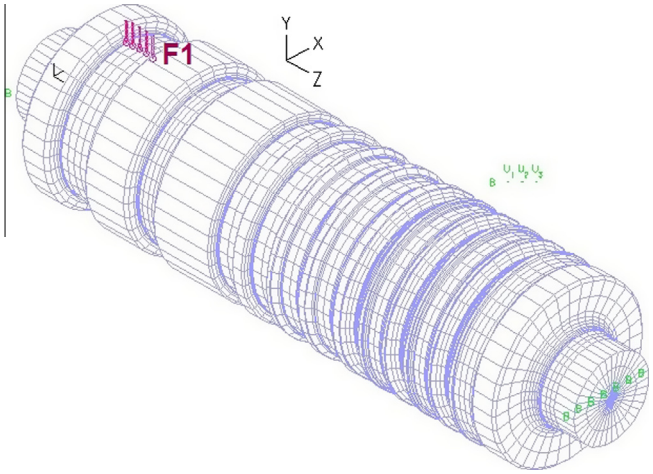

Fig. 7. Linear elastic model with 3D solid elements.

Stress time history of the individual local stress and stress spectra are obtained from numerical analysis and rolling schedule according to time, Fig. 13.

Fatigue strength of the roll material in the pass groove was missing and fatigue strength was determined by experimental testing. From the new roll, dimensions ⌀500 × 1500 mm with same characteristics as in rolls in service, one ring dimensions ⌀440 × ⌀320 × 170, Fig. 10, was taken out by turning. The hardness measurements were done in four places.

Specimens, (as shown) in Fig. 11, were taken from the ring by water cutting. Final testing shape of the specimen was achieved by a grinding machine. During the grinding, specimens were cooled with lot of water to avoid material losing its properties. Fig. 12 shows metallographic structure of specimen.

Dynamic tests were carried out in Laboratory of fatigue strength at Department of Mechanical Construction, Faculty of Electrical Engineering, Mechanical Engineering and Naval Architecture, University of Split. Bending tests were performed on the plane bending mechanical testing machine. The fatigue strength was determined after complete failure of 24 specimens in high cycle regime (10,000–1,000,000 cycles). Additional 24 specimens were tested

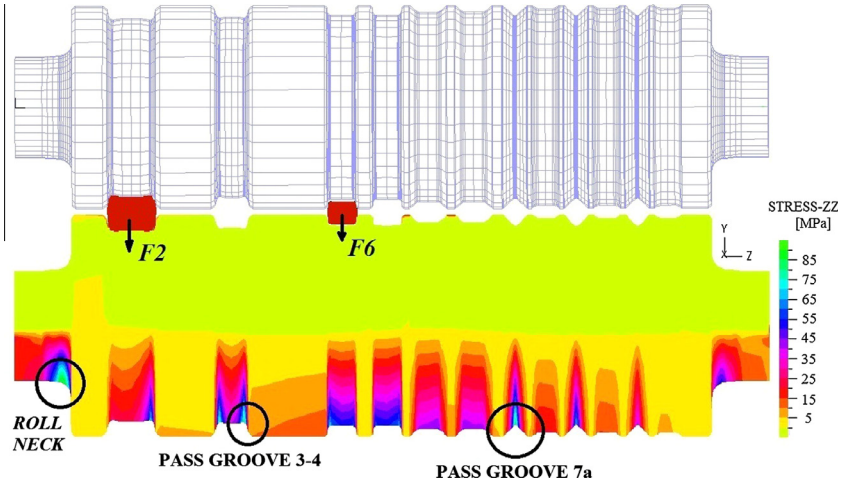

Fig. 8. Numerical analysis.

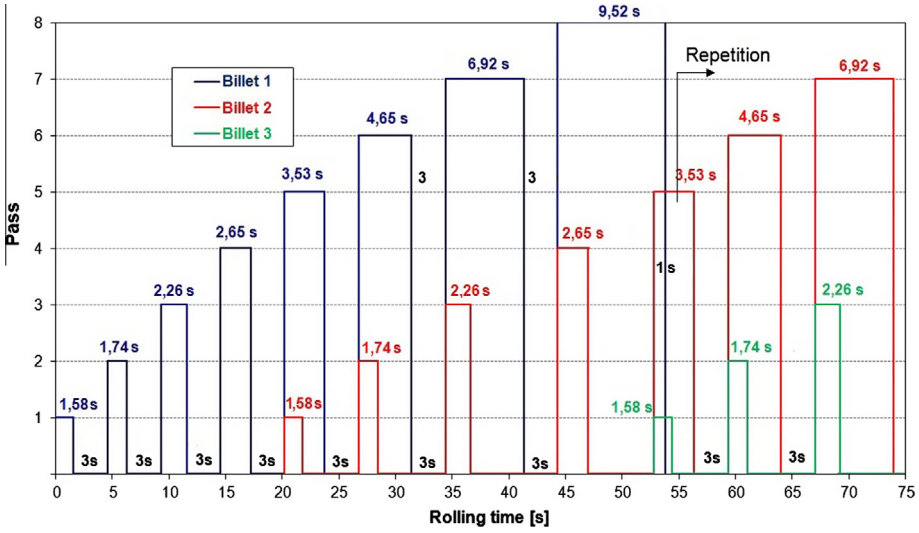

Fig. 9. Rolling schedule according to time on 3-high-roughing mill stand.

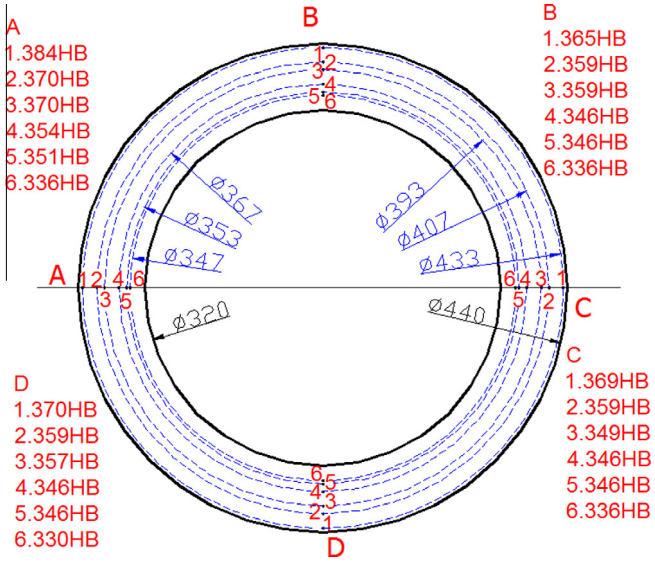

Fig. 10. Ring was taken from the new roll in order to prepare specimens.

in servo-hydraulic fatigue test machine (tension), and these results are very similar with results obtained in bending.

Fig. 13 shows experimentally obtained fatigue strength of the roll material under constant amplitude in the pass groove (with all parameters of the tests and probability *S–N* curves) as well as stress spectra of three critical areas: on the roll neck, pass groove 3–4 and pass groove 7a for 4000 rolling tons.

From the comparison of the presented spectra it can be seen that the most critical area of the roll is pass groove 7a. Because of that an analysis of the influences of the rolling temperature, rolling speed, roll design and turning due to wearing on roll fatigue life was carried out on the pass groove 7a.

2. Influence of rolling temperature on fatigue life

In order to reduce the cost of energy, an analysis of the rolling temperature influence on roll fatigue life was carried out for 3 different initial rolling temperatures: 1200 °C, 1150 °C and 1100 °C. Resistance to deformation for 3 different initial temperatures in each pass is determined from diagram of A.A.Dinnik, Fig. 3. The results are shown in Table 4.

Based upon the results of experimental determination of rolling forces, methods of Tselikov, Korolev, Sims and Siebel were used to calculate rolling forces for 3 different initial rolling temperatures and values are shown in Table 5.

Rolling force increments due to decreasing initial rolling temperature are shown in Table 6.

Based on this data it is obvious that the rolling forces increment is about 15% for decreasing initial rolling temperature from 1200 °C to 1150 °C and about 30% for decreasing initial rolling temperature from 1200 °C to 1100 °C. The obtained experimental values of rolling forces with an increase of 15% and 30% are used for numerical analysis of local stresses. Stress spectra for the initial rolling temperatures 1150 °C and 1100 °C determined from numerical analysis and pass schedule are shown on the Fig. 14.

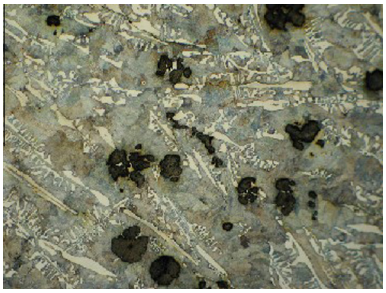

Fig. 12. Metallographic structure of specimen (500×).

Decrease of initial rolling temperature from 1200 °C to 1150 °C reduces the fatigue life of the roll about 40%; decrease from 1200 °C to 1100 °C causes reduction about 60%.

3. Influence of rolling speed on fatigue life

In order to increase rolling production, an analysis of the rolling speed influence on the fatigue life of the rolls has been carried out for 3 different roll speeds: 120 rpm, 150 rpm and 180 rpm. Resistance to deformation for 3 different roll speeds in each pass is determined from diagram of A.A.Dinnik, Fig. 3. The results are shown in Table 7.

The rolling forces for 3 different speeds were calculated according to Tselikov, Korolev, Sims and Siebel methods and values of rolling forces are shown in Table 8.

Rolling force increments due to roll speed increasing are shown in Table 9.

It is obvious that the rolling forces increment is about 3% for increasing roll speed from 120 rpm to 150 rpm and about 6% for increasing roll speed from 120 rpm to180 rpm. The obtained experimental values of rolling forces with an increase of 3% and 6% are used for numerical analysis of local stresses. Stress spectra for the roll speeds 150 rpm and 180 rpm determined from numerical analysis and rolling schedule are shown in Fig. 15.

Increasing rolling speed from 120 rpm to 150 rpm reduces the fatigue life of the roll for about 11% and increasing rolling speed from 120 rpm to 180 rpm reduces the fatigue life of the roll for about 19%.

4. Influence of roll groove design on fatigue life

In order to reduce stress concentration on the critical area, an analysis of square shape design was carried out. The square pass design is limited by technological rules of rolling [2,3]. Small change of groove angle changes square shape in diamond shape.

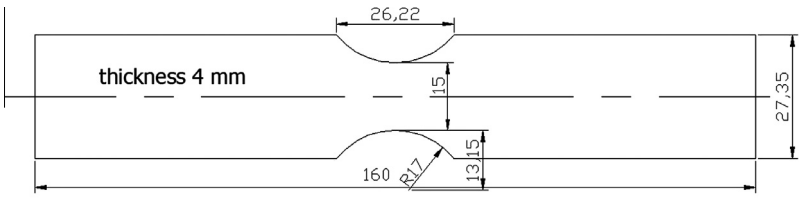

Fig. 11. Shape and dimensions of the specimen.

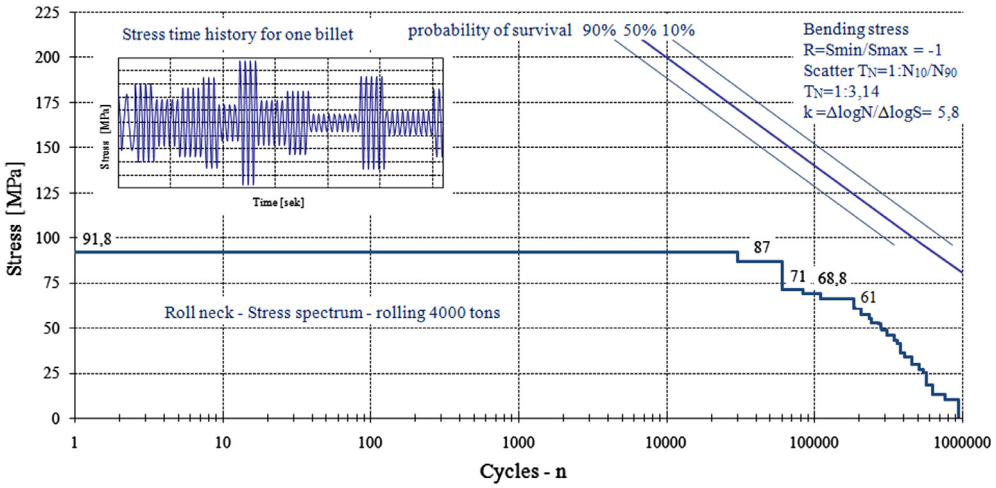

(a) Roll neck

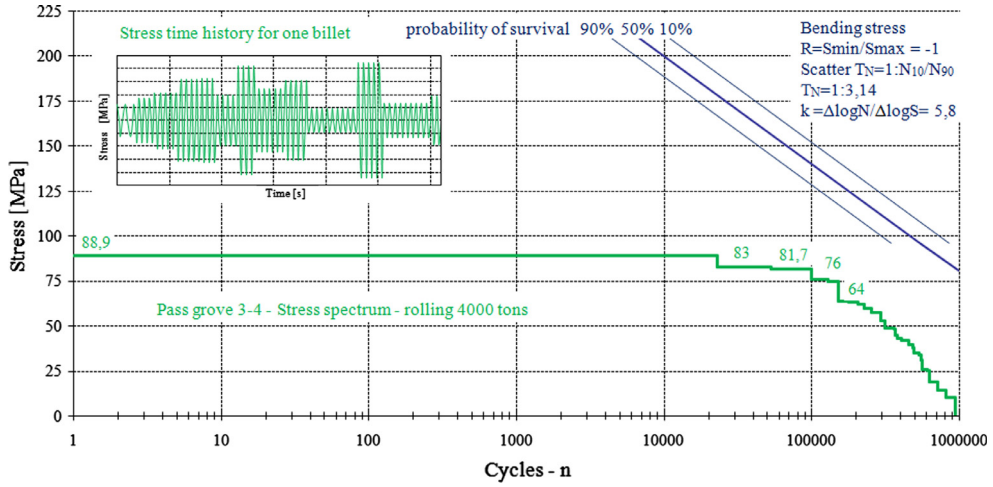

(b) Pass groove 3-4

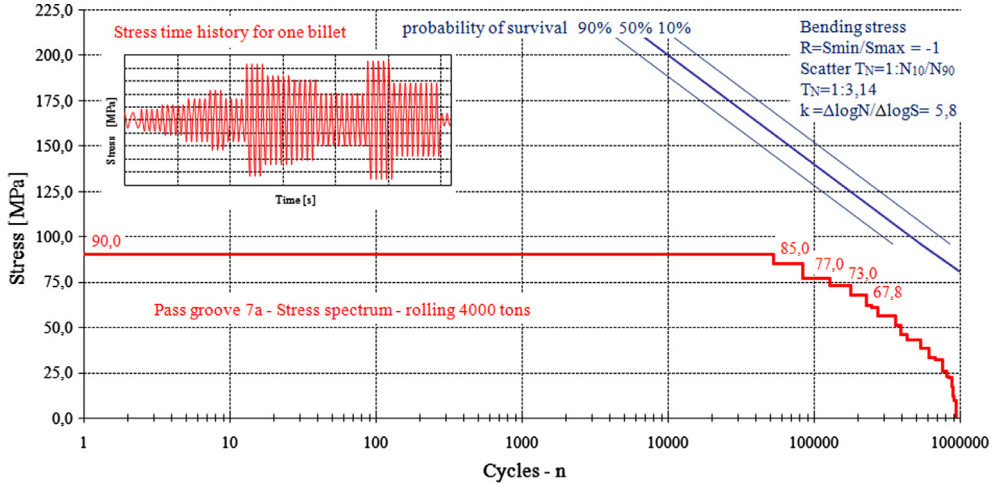

(c) Pass groove 7a

Fig. 13. Stress spectra for critical areas.

Because of that, square pass design can be changed by changing the size of radius in the groove bottom. The radius in the groove bottom can be $r_1 = (0.1–0.2)\ a$, and a is square size, Fig. 16.

For the pass 7a, see Fig. 17, the radius in the bottom of the groove was increased from 6 mm to 8 mm. The experimental results of rolling forces were used for the numerical analysis of local stresses. The FEM revealed that increasing the radius from

Table 4
Resistance to deformation in the passes for different initial temperature.

Pass No.	0	1	2	3	4	5	6	7	8
Rolling temperature (°C)	1200	1198	1194	1188	1183	1176	1169	1159	1146
Resistance to deformation t_0 = 1200 °C (N/mm^2)		66.3	75.5	64.5	83.0	73.6	89.8	86.8	98.1
Rolling temperature (°C)	1150	1148	1144	1138	1133	1126	1119	1109	1096
Resistance to deformation t_0 = 1150 °C (N/mm^2)		76.0	86.4	73.6	94.7	83.8	102.1	98.3	110.8
Rolling temperature (°C)	1100	1098	1094	1088	1083	1076	1069	1059	1046
Resistance to deformation t_0 = 1100 °C (N/mm^2)		85.7	97.4	82.8	106.5	93.9	114.4	109.8	123.5

Table 5
Rolling forces calculation for 3 different temperatures in the first pass.

Pass No.		1	2	3	4	5	6	7	8
Rolling temperature (°C)	1200	1198	1194	1188	1183	1176	1169	1159	1146
Rolling forces Tselikov F1200 (kN)		430.7	506.3	377.9	510.3	364.2	518.4	342.8	473.7
Rolling forces Koroljev F1200 (kN)		436.0	510.5	387.8	517.2	370.4	515.2	352.3	451.6
Rolling forces Sims F1200 (kN)		384.0	508.1	367.7	501.2	363.5	517.0	347.1	462.5
Rolling forces Siebel F1200 (kN)		391.2	516.2	366.1	521.7	361.9	538.1	330.6	460.5
Rolling temperature (°C)	1150	1148	1144	1138	1133	1126	1119	1109	1096
Rolling forces Tselikov F1150 (kN)		497.6	585.0	436.0	589.4	420.4	600.0	394.4	550.6
Rolling forces Koroljev F1150 (kN)		502.7	588.5	445.8	595.1	425.3	592.3	402.7	517.9
Rolling forces Sims F1150 [kN]		440.3	581.8	419.9	572.1	413.7	587.7	392.9	522.4
Rolling forces Siebel F1150 (kN)		448.4	591.1	418.1	595.5	411.9	611.8	374.2	520.1
Rolling temperature (°C)	1100	1098	1094	1088	1083	1076	1069	1059	1046
Rolling forces Tselikov F1100 (kN)		565.5	665.1	495.1	670.1	478.0	684.3	447.5	631.4
Rolling forces Korolev F1100 (kN)		570.1	667.5	504.6	674.1	481.2	671.1	453.9	585.9
Rolling forces Sims F1100 (kN)		496.5	655.5	472.1	643.0	463.9	658.5	438.8	582.3
Rolling forces Siebel F1100 (kN)		505.7	666.0	470.1	669.3	461.9	685.4	417.9	579.8

Table 6
Force increment.

Pass No.	1	2	3	4	5	6	7	8	Average
Tselikov F1150/F1200	1.16	1.16	1.15	1.15	1.15	1.16	1.15	1.16	1.16
Koroljev F1150/F1200	1.15	1.15	1.15	1.15	1.15	1.15	1.14	1.15	1.15
Sims F1150/F1200	1.15	1.15	1.14	1.14	1.14	1.14	1.13	1.13	1.14
Siebel F1150/F1200	1.15	1.15	1.14	1.14	1.14	1.14	1.13	1.13	1.14
Tselikov F1100/F1200	1.31	1.31	1.31	1.31	1.31	1.32	1.31	1.33	1.32
Koroljev F1100/F1200	1.31	1.31	1.30	1.30	1.30	1.30	1.29	1.30	1.30
Sims F1100/F1200	1.29	1.29	1.28	1.28	1.28	1.27	1.26	1.26	1.28
Siebel F1100/F1200	1.29	1.29	1.28	1.28	1.28	1.27	1.26	1.26	128

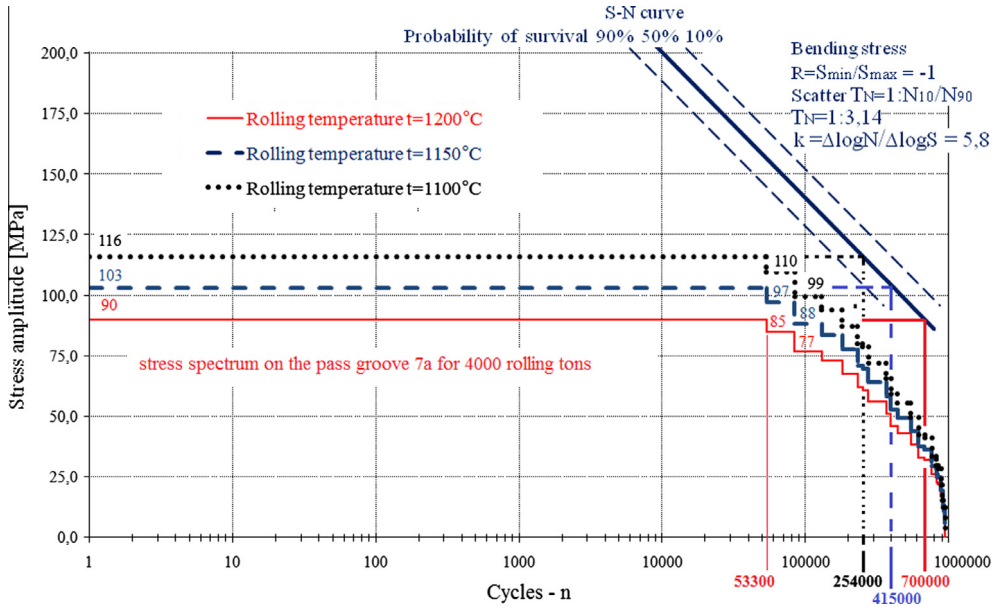

Fig. 14. Influence of rolling temperature on fatigue life.

Table 7
Resistance to deformation in the passes for different roll speeds.

Roll speed (rpm)	Pass No.	1	2	3	4	5	6	7	8
120	Rolling speed (ms^{-1})	2.33	2.62	2.42	2.77	2.55	2.78	2.7	2.89
120	Deformation speed (s^{-1})	7.9	9.5	7.4	12.0	9.6	15.5	10.5	18.7
120	Resistance to deformation (N/mm^2)	66.3	75.5	64.5	83	73.6	89.8	86.8	98.1
150	Rolling speed (ms^{-1})	2.92	3.28	3.03	3.46	3.19	3.47	3.38	3.61
150	Deformation speed (s^{-1})	9.9	11.9	9.2	14.9	12.0	19.4	13.1	23.4
150	Resistance to deformation (N/mm^2)	68.6	78.1	66.7	85.8	76.1	92.9	88.9	101.6
180	Rolling speed (ms^{-1})	3.50	3.93	3.63	4.15	3.83	4.17	4.06	4.33
180	Deformation speed (s^{-1})	11.8	14.3	11.0	17.9	14.4	23.2	15.7	28.1
180	Resistance to deformation (N/mm^2)	70.5	80.2	68.6	88.2	78.3	95.5	92.4	104.4

Table 8
Rolling forces calculation for 3 different roll speeds.

Roll speed (rpm)	Pass No. (kN)	1	2	3	4	5	6	7	8
120	Rolling forces Tselikov F120	430.7	506.3	377.9	510.3	364.2	518.4	342.8	473.7
120	Rolling forces Koroljev F120	436.0	510.5	387.8	517.2	370.4	515.2	352.3	451.6
120	Rolling forces Sims F120	384.0	508.1	367.7	501.2	363.5	517.0	347.1	462.5
120	Rolling forces Siebel F120	391.2	516.2	366.1	521.7	361.9	538.1	330.6	460.5
150	Rolling forces Tselikov F150	445.4	523.6	390.9	527.9	376.8	536.3	354.7	490.3
150	Rolling forces Koroljev F150	450.9	528.0	401.1	535.0	383.2	533.1	364.6	467.4
150	Rolling forces Sims F150	397.2	525.5	380.3	518.5	376.1	534.9	359.2	478.7
150	Rolling forces Siebel F150	404.6	533.9	378.7	539.7	374.4	556.8	342.1	476.6
180	Rolling forces Tselikov F180	457.8	538.2	401.8	542.7	387.4	551.5	364.8	504.3
180	Rolling forces Korolev F180	463.5	542.8	412.3	550.1	394.0	548.1	374.9	480.8
180	Rolling forces Sims F180	408.2	540.1	391.0	533.0	386.6	550.0	369.4	492.3
180	Rolling forces Siebel F180	415.8	548.8	389.3	554.8	385.0	572.5	351.8	490.2

Table 9
Force increment.

Pass No.	1	2	3	4	5	6	7	8	Average
Tselikov F150/F120	1.03	1.03	1.03	1.03	1.03	1.03	1.03	1.04	1.03
Koroljev F150/F120	1.03	1.03	1.03	1.03	1.03	1.03	1.03	1.04	1.03
Sims F150/F120	1.03	1.03	1.03	1.03	1.03	1.03	1.03	1.04	1.03
Siebel F150/F120	1.03	1.03	1.03	1.03	1.03	1.03	1.03	1.04	1.03
Tselikov F110/F120	1.06	1.06	1.06	1.06	1.06	1.06	1.06	1.06	1.06
Koroljev F110/F120	1.06	1.06	1.06	1.06	1.06	1.06	1.06	1.06	1.06
Sims F110/F120	1.06	1.06	1.06	1.06	1.06	1.06	1.06	1.06	1.06
Siebel F110/F120	1.06	1.06	1.06	1.06	1.06	1.06	1.06	1.06	1.06

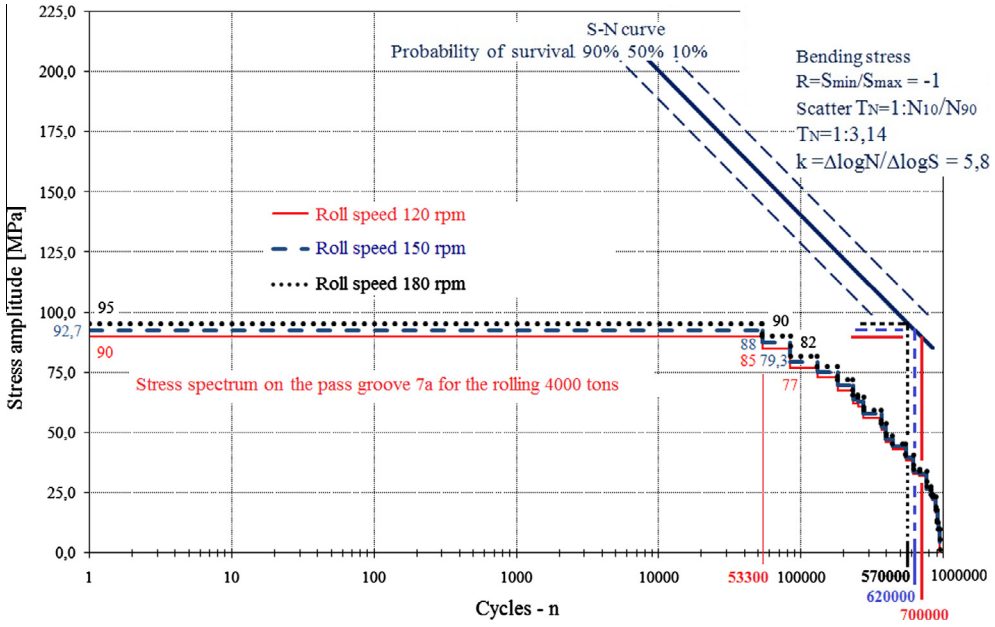

Fig. 15. Influence of rolling speed on fatigue life.

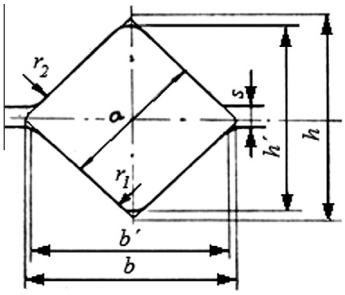

Fig. 16. Square shape design.

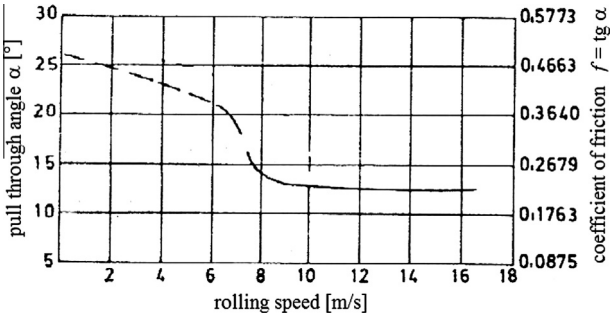

Fig. 19. Pull through angle of low carbon steel with 0.18% C, Z. and R. Wusatowski, [2].

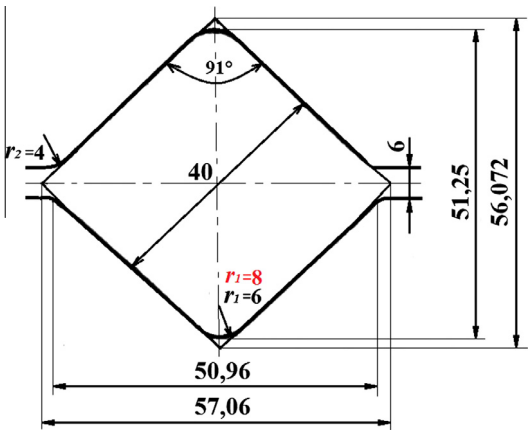

Fig. 17. Design of pass 7a.

6 mm to 8 mm decreases maximum local stress about 4%. Reducing the size of radius will increase stresses. Stress spectrum for radius 8 mm in the groove bottom is determined from numerical analysis and rolling schedule, see Fig. 18. The change of radii size from 6 to 8 mm in the groove bottom increases the fatigue life 12%.

5. Influence of roll groove height on fatigue life

Additionally, roll groove height was analyzed to reduce the maximum stresses on the critical areas. The size of groove height is controlled by maximum draught (difference between initial height and height after pass). Maximum draught in the passes is

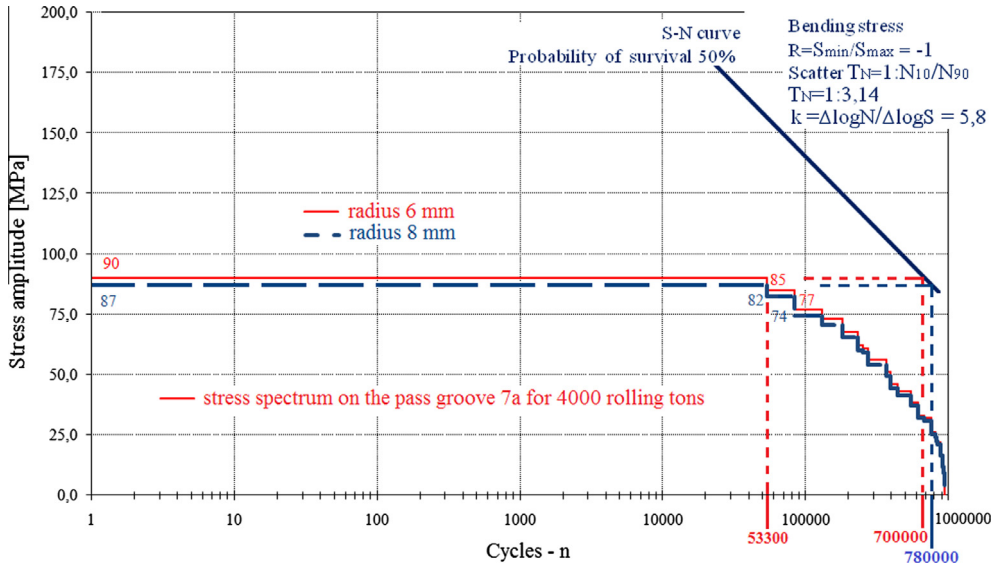

Fig. 18. Influence of shape detail in the pass groove on fatigue life.

Table 10
Maximum draught in passes.

Pass		1	2	3	4	5	6	7
Rolling speed (ms^{-1})	2.33	2.62	2.42	2.77	2.55	2.78	2.7	2.89
Maximum pull through angle – α_{max}	24	24	24	23.5	24	23.5	23.5	23
Maximum draught – Δh_{max} (mm)	32.3	34	32.3	32.9	34.4	34.7	32.8	34.4

Table 11
Pass schedule for new desing.

Pass		1	2	3	4	5	6	7	8
Pass shape		Box	Box	Box	Box	Box	Oval	Square	Oval
Groove dimensions (mm)		100 × 82	100 × 66	67 × 80	67 × 59	66 × 52	80 × 34	40	58 × 20
Width (mm)	100	104	108	71	76	65	82.5	53.5	60.5
Initial height (mm)		100	80	108	78	76	48	82.5	40.0
Height after pass (mm)		80	66	78	61	48	34	51	22.5
Draught (mm)		20	14	30	17	28	14	31.5	17.5

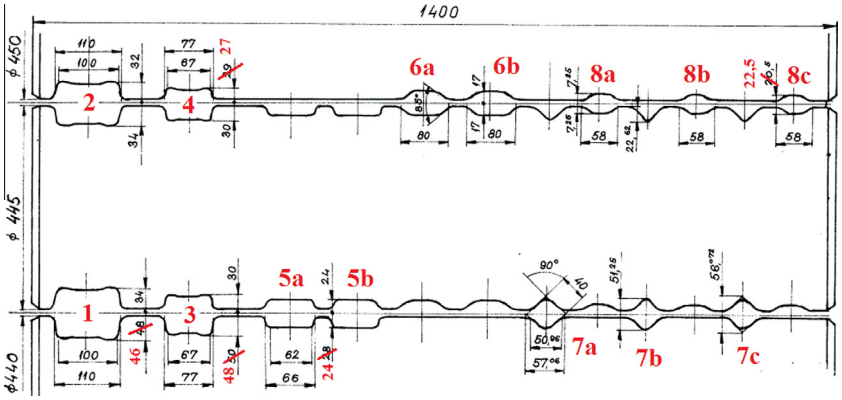

Fig. 20. Changes of pass heights in roll groove design.

Table 12
Rolling forces calculation for new roll groove design.

Pass No.	1	2	3	4	5	6	7	8
Rolling forces Tselikov – basic design (kN)	430.7	506.3	377.9	510.3	364.2	518.4	342.8	473.7
Rolling forces Tselikov – new design (kN)	458.0	498.5	388.7	492.5	396.6	480.0	342.8	456.4
Coefficient of force change – Tselikov	1.06	0.93	1.03	0.91	1.09	0.88	1.00	0.91
Rolling forces Korolev –basic design (kN)	436.0	510.5	387.8	517.2	370.4	515.2	352.3	451.6
Rolling forces Korolev – new design (kN)	464.8	501.5	400.2	496.6	405.7	475.2	352.3	438.4
Coefficient of force change – Korolev	1.07	0.93	1.03	0.91	1.10	0.87	1.00	0.92
Rolling forces Sims – basic design (kN)	384.0	508.1	367.7	501.2	363.5	517.0	347.1	462.5
Rolling forces Sims – new design (kN)	406.5	502.2	381.7	475.6	401.6	484.5	347.1	460.1
Coefficient of force change – Sims	1.06	0.94	1.04	0.90	1.10	0.89	1.00	0.94
Rolling forces Siebel – basic design (kN)	391.2	516.2	366.1	521.7	361.9	538.1	330.6	460.5
Rolling forces Siebel – new design (kN)	414.1	510.3	380.1	495.1	399.8	504.3	330.6	458.1
Coefficient of force change – Siebel	1.06	0.94	1.04	0.90	1.10	0.89	1.00	0.94
Average coefficient from all four authors	1.06	0.93	1.03	0.91	1.10	0.88	1.00	0.93
Experimentally determined rolling forces (kN)	356.1	494.6	356.1	524.2	346.2	544.0	286.8	445.1
Calculated rolling forces for new design	378.0	462.4	368.3	475.0	380.3	479.9	286.8	413.7

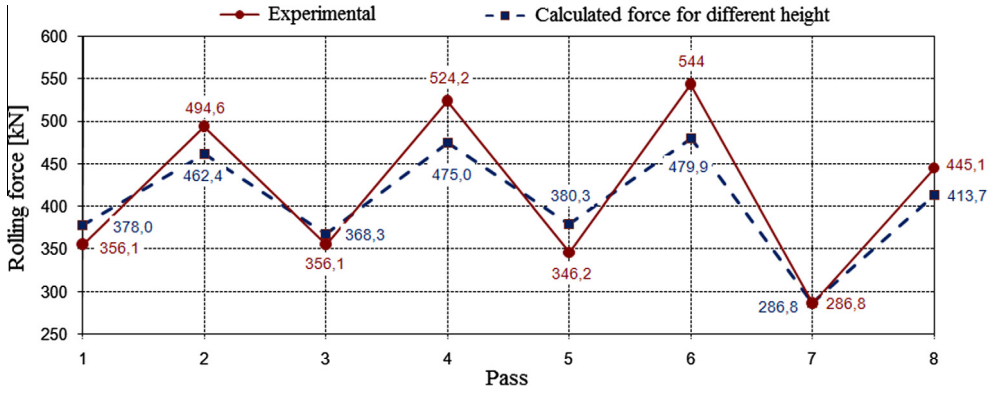

Fig. 21. Rolling forces after change of pass heights.

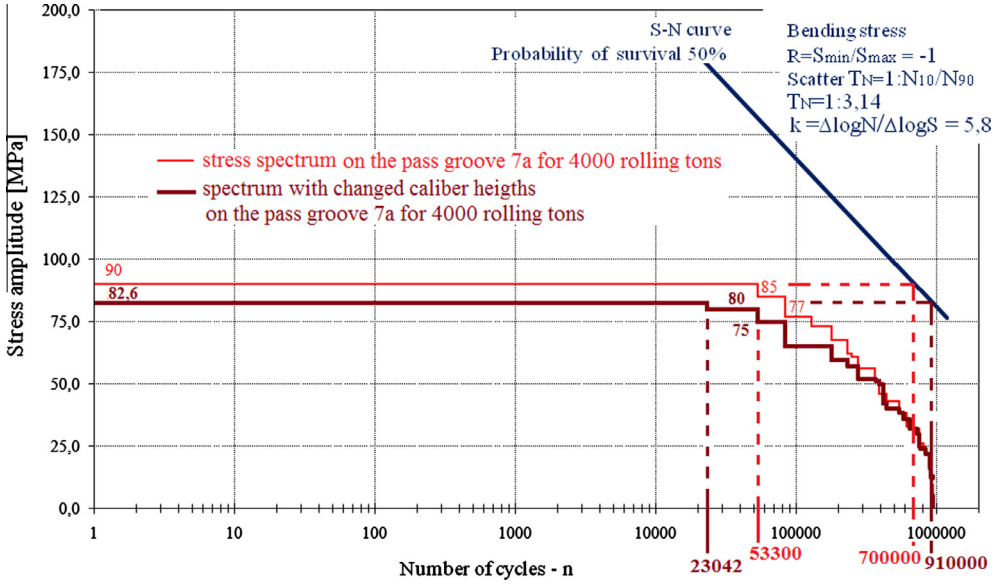

Fig. 22. Influence of pass heights in roll groove design on fatigue life.

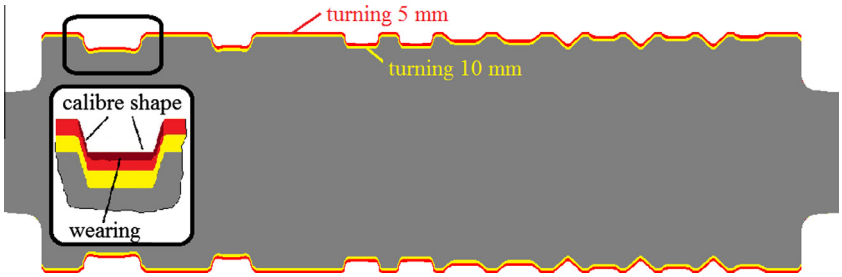

Fig. 23. Roll turning due to wearing.

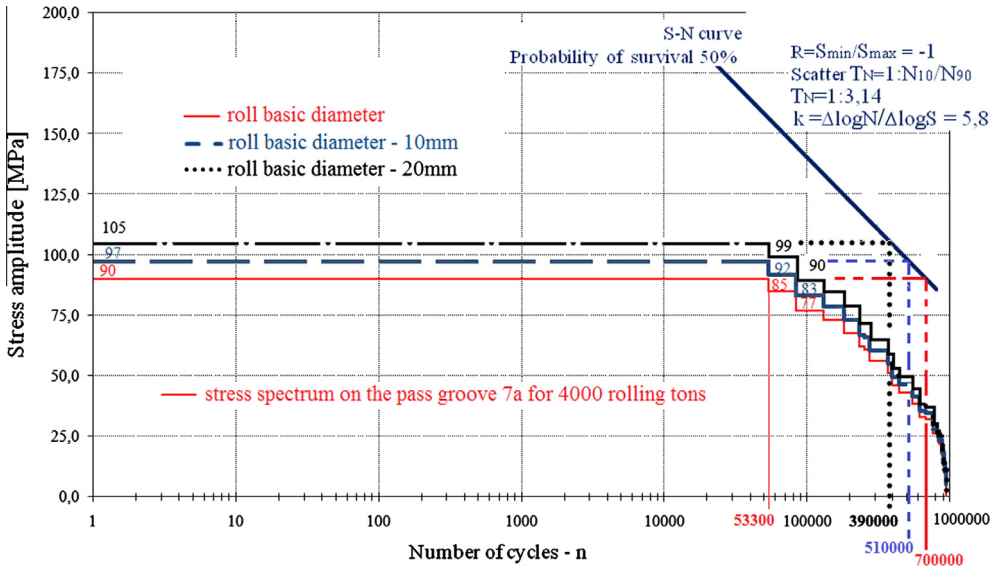

Fig. 24. Influence of turning due to wearing on fatigue life.

determined in accordance with relation [2,3], as shown in Table 10:

$$\Delta h_{max} = D \cdot \left(1 - \frac{1}{\sqrt{1 + tg^2 \alpha_{max}}}\right) \quad (2)$$

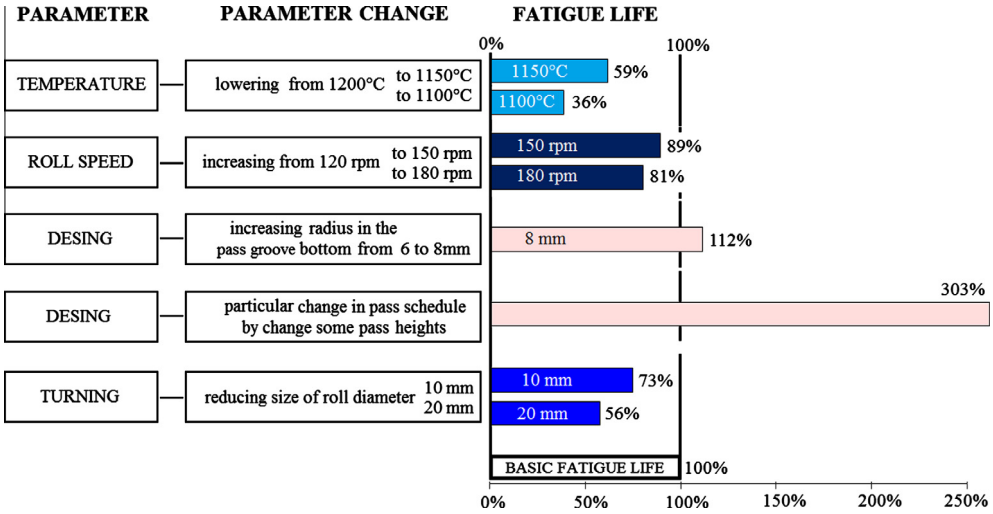

Fig. 25. Results overview.

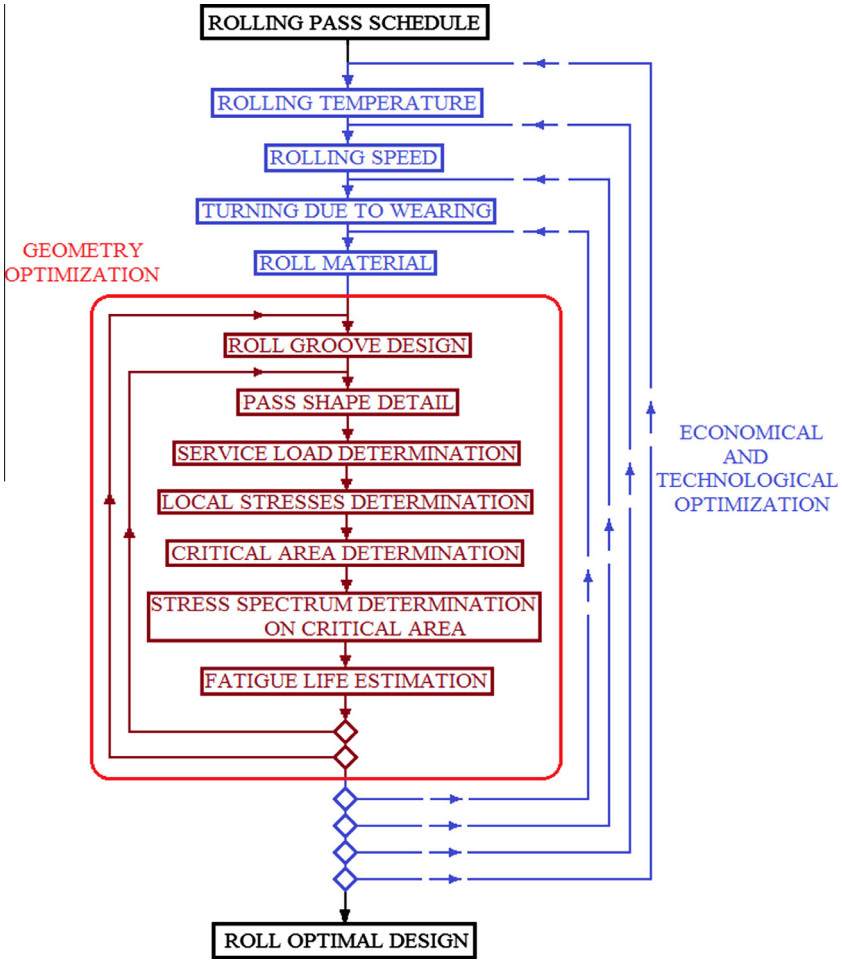

Fig. 26. Procedure for optimal fatigue design of calibrated rolls.

where D is the diameter of the roll and α is pull through angle in the pass.

Experimentally obtained diagram of Z. and R. Wusatowski [2], shown in Fig. 19 is used for the estimation of maximum pull

through angle in the passes. Maximum draught in passes is shown in Table 10.

From the Fig. 6 it can be seen that the rolling forces in passes 2, 4, 6 and 8 are higher than in the passes of 1, 3, 5 and 7 and maximum stresses occur during rolling in passes 2 and 6 and passes 4 and 8. Based on this fact, the size of the groove height was changed, see Table 11. The Fig. 20 shows the changes of pass heights in roll groove design.

The rolling forces for the new roll groove design were calculated according to Tselikov, Korolev, Sims and Siebel methods and results are shown in Table 12 and Fig. 21.

The calculated rolling forces shown in Table 12 are used for the numerical analysis of local stresses. Stress spectrum for pass 7a is determined from numerical analysis and rolling schedule. Stress spectra comparison for two pass schedules with different pass heights are shown in Fig. 22. It may be seen that small change of the pass height can increase fatigue life several times.

6. Influence of turning due to wearing on fatigue life

During service life, roll grooves lose requested pass shape due to wearing. When grooves are worn, Fig. 23, the roll should be machined by turning machine.

After turning, the size of the roll diameter is smaller. The influence of turning due to wearing on fatigue life is shown in Fig. 24. Reducing the size of the roll diameter reduces the fatigue life of the roll about 27% for 10 mm and about 44% for 20 mm.

7. Results

An analysis of influence the rolling temperature, rolling speed, design and turning due to wearing on roll fatigue life was done in order to increase the maximum fatigue life of the rolls, reduce overall energy consumption, increase production and reduce overall costs. All parameters were changed according to technological limits. The overview of the results is shown in Fig. 25.

Fig. 25 shows that design geometry and resulting stress distribution in highly stressed area are a decisive factor influencing the fatigue life of the rolls. In order to reduce energy consumption by reducing rolling temperature and increase production by increasing rolling speed with proper design, their negative influences can be compensate.

Based on the shown analysis and results, the developed procedure for optimal fatigue design of calibrated rolls is shown in Fig. 26.

The first task in shown procedure is the determination of service load for the roll, in this case rolling forces, by analytical or experimental methods. The obtained results of the rolling forces are used for numerical analysis of the local stresses by the finite element method to find the most critical highly stressed area of the rolls. The next step was to determine stress spectrum on the critical area according to pass schedule and corresponding stresses. The estimation of the fatigue life was carried out by comparing the spectrum of stress at the critical location and S–N curve obtained from roll material under constant amplitude testing. This routine should be repeated till requested fatigue life is reached.

The first parameter which should be changed is the structural detail of the pass shape at critical location. The structural detail of the pass shape can be changed during the roll turning and therefore does not entail any additional costs. In this way, the maximum fatigue life can be achieved by individual changing at every critical place.

The next parameter which should be changed is the pass schedule. Re-arranging pass schedule can be achieved in two ways: by changing the pass height or changing pass shape and pass arrangement. The pass height can be also changed during the roll turning, and therefore it does not entail any additional cost. For some small change of the pass shape and pass arrangement, the cost is negligible. The change of pass shape and pass arrangement usually requires different design of the rolls with completely different geometry, different load distribution and corresponding stresses. Therefore, this change requires a completely new assessment of fatigue life with significant structural changing of auxiliary equipment.

The third parameter is material. The use of materials more resistant to dynamic loads usually means increasing cost for the rolls and hence increasing overall costs as well.

The last parameters in this procedure are rolling temperature and rolling speed. Reducing rolling temperature and increasing rolling speed provide reduction in costs and increase production, but the effect of these changing on fatigue life is negative. This negative effect can be compensated with proper design. Changing of these technological parameters should follow economic feasibility analysis.

The final result of proposed procedure is an optimal roll design according to roll fatigue life on one side and energy consumption, production and overall costs on the other side, for given initial conditions. In this paper, the proposed procedure is developed for hot rolling process, but this could also be applicable for other metal working processes (for e.g. forging); those will be the directions of future research.

References

[1] Lukša F. Methodology of constructing optimal calibrated rolls with respect to fatigue life. Doctor Thesis, University of Split, Faculty of Electrical Engineering, Mechanical Engineering and Naval Architecture, Split; 2012.
[2] Čaušević M. Obrada metala valjanjem. Sarajevo: Veselin Masleša; 1983.
[3] Čaušević M. Valjanje i kalibriranje. Beograd: Tehnička knjiga; 1962.
[4] Designs and technological rules "Steelworks Split", Split.
[5] Valji d.o.o., Štore, Cast Iron rolls, catalog.
[6] Lukša F. Investigation of the cause of the failures of the rolls with grooves. Master Thesis, University of Split, Faculty of Electrical Engineering, Mechanical Engineering and Naval Architecture, Split; 2005.
[7] Domazet Ž, Lukša F. Experimental determination of the rolling force on the rolls with grooves. In: Proceedings of the 22-nd symposium "DANUBIA-ADRIA" on experimental methods in solid mechanics, Parma; 2005.
[8] Pilkey WD, Pilkey DF. Stress concentration factors. 3rd ed. Hoboken, New York: John Wiley & Sons; 2008.
[9] Heibach E. Betriebfestigkeit. Düseldorf: VDI Verlag Gmbh; 1989.